# Directed evolution of angiotensin-converting enzyme 2 (ACE2) variants with enhanced peptidase activity profiles for novel therapeutic applications

**Authors**

Pete Heinzelman[1] and Philip A. Romero[1,2*]

[1]Department of Biochemistry, University of Wisconsin-Madison, Madison, WI, USA. [2] Department of Chemical & Biological Engineering, University of Wisconsin-Madison, Madison, WI, USA. *Correspondence: promero2@wisc.edu

**Author contributions**

P.H. and P.A.R conceived the project. P.H. performed the experiments. P.H. and P.A.R analyzed the data. P.H. and P.A.R. wrote the manuscript.

**Competing Interest Statement**

P.H. and P.A.R are pursuing a patent related to ACE2 variants with modified catalytic activity and specificity profiles.

**Keywords**

acute respiratory distress syndrome
angiotensin converting enzyme 2
yeast surface display

**Abstract**

Mutants of the Angiotensin Converting-Enzyme 2 (ACE2) carboxypeptidase possessing enhanced hydrolytic activity and specificity hold potential to beneficially modulate the Angiotensin receptor (ATR) therapeutic axis with increased efficacy and reduced potential side effects relative to wild type ACE2. In pursuing this goal, we established a yeast display-based liquid chromatography screen that enabled use of directed evolution to identify ACE2 mutants with improved target peptide substrate, Angiotensin-II (Ang-II), activity and specificity relative to Apelin-13, an off-target peptide substrate.

Screening yeast-displayed ACE2 active site residue saturation mutant libraries revealed three substitution-tolerant positions that can be mutated to enhance ACE2's activity profile. Double mutant libraries combining substitutions at these positions, M360, T371 and Y510, yielded candidate improved ACE2 mutants that were recombinantly expressed and purified at 1 mg/L yield and > 90% homogeneity.

Relative to wild type, the leading mutant, T371L/Y510Ile, has seven-fold increased $k_{cat}$ toward Ang-II and six-fold decreased $k_{cat}/K_m$ for Apelin-13 hydrolysis. In single substrate hydrolysis assays featuring physiologically relevant substrate concentrations T371L/Y510Ile hydrolyzes more Ang-II than wild type with concomitant Ang-II:Apelin-13 specificity improvements reaching 30-fold. Additionally, T371L/Y510Ile hydrolyzed Ang-II at rates greater than wild type, with Apelin-13 hydrolysis reductions of up to 80 percent, in multiplex assays containing a mixture of peptides relevant to the ATR therapeutic axis. Our efforts have delivered ATR axis-acting therapeutic candidates with relevance to established and unexplored ACE2 therapeutic applications and demonstrate the feasibility of developing ACE2 variants for use in biomedical contexts unrelated to the ATR axis such as localized activation of peptide-based prodrugs.

**Significance Statement**

The Angiotensin Converting Enzyme 2 (ACE2) carboxypeptidase is being clinically trialed for treatment of acute respiratory distress syndrome (ARDS) related to traumatic injuries and viral infections. We developed a yeast display-based directed evolution method that enabled isolation of mutant ACE2s possessing enhanced peptide substrate hydrolysis activity and specificity profiles with respect to substrates relevant to ARDS. Beyond their potential utility as ARDS therapeutics, our improved ACE2 variants could have an impact in unexplored ACE2 therapeutic contexts such as treating Alzheimer's Disease. Our directed evolution method has also created an opportunity to develop ACE2 mutants that specifically hydrolyze nonnative peptide sequences; such variants could give rise to additional novel ACE2 biomedical applications including targeted activation of peptide-based prodrugs for cancer therapy.

## Introduction

Angiotensin-Converting Enzyme 2 (ACE2) is a zinc-dependent mono-carboxypeptidase found in both membrane bound and freely circulating forms *in vivo* [1]. ACE2's ability to hydrolyze the Angiotensin-II peptide, a substrate whose hydrolysis is associated with salutary blood flow increase [2], suppression of inflammation [3] and attenuation of pathological tissue remodeling after acute injury [2], has motivated pursuit of ACE2 as an agent for treating respiratory viral infections [4], acute respiratory distress syndrome [5], diabetes [6]. ACE2's utility in both treating these conditions and in unexplored biomedical arenas including Alzheimer's Disease therapy [7] and localized *in vivo* activation of peptide-based prodrugs [8] has been limited by the fact a substantial number, where at least eight peptides found in circulation and/or tissues *in vivo* have been identified as ACE2 substrates [9,10], of peptides are hydrolyzed by this enzyme.

Apelins, which exist in isoforms of varying amino acid lengths and share a C-terminus recognized by ACE2, are the ACE2 peptide substrates for which potential avenues by which increased ACE2-mediated hydrolysis *in vivo* could lead to deleterious side effects, in particular myocardial dysfunction, have been most well-defined [9,11]. Additionally, ACE2's catalytic efficiency, i.e., $k_{cat}/K_m$, toward Ang-II is similar to its efficiency toward Apelins [10,11] and the concentration of Apelins, which are present at single-digit nM levels in human plasma [12], are higher than both the 10-50 pM Ang-II concentrations observed in blood [13,14] and the 0.2-0.3 nM levels of Ang-II found in human tissues [13,15]; these observations support the hypothesis that Apelins can be potent competitors of ACE-2 activity toward Ang-II under the mixed peptide substrate conditions that exist *in vivo*. Taken together, the above statements motivate identification of ACE2 mutants with greater than wild type Ang-II:Apelin hydrolytic activity ratios, and ideally equal to or greater than wild type Ang-II hydrolytic activity, as an ACE2-based therapeutic development objective (Figure 1).

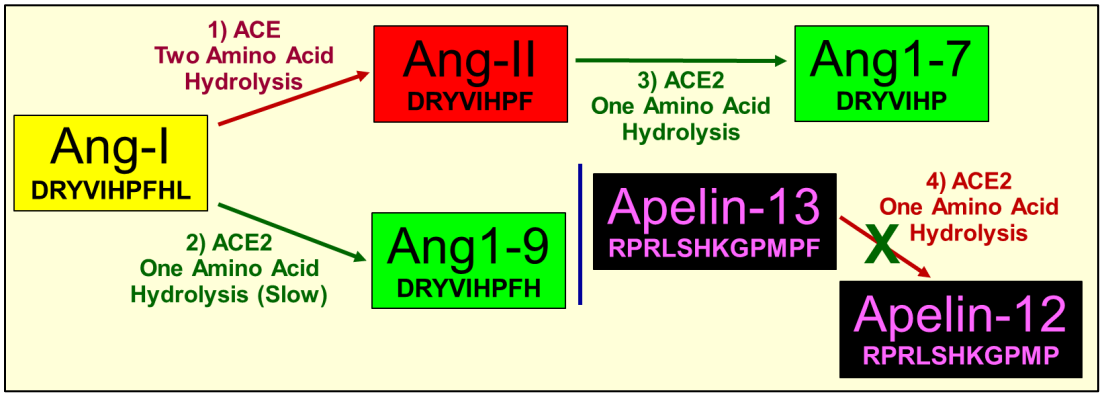


**Figure 1.** Key peptidase reactions relevant to Ang-II/ATR/MasR therapeutic axis. Red arrows denote hydrolysis reactions with known or potentially undesirable *in vivo* effects. Green arrows denote hydrolysis reactions with established or posited beneficial effects. 1. ACE dipeptidase removes two C-terminal residues (His-Leu) from Ang-I to yield Ang-II. 2. ACE2 removes C-terminal Leu from Ang-I to produce Ang1-9 (very slow relative to reactions 1 and 3). 3. ACE2 removes C-terminal Phe from Ang-II to produce Ang1-7. 4. ACE2 removes C-terminal Phe from Apelin-13 to yield Apelin-12; blue X denotes desirability of ACE2 variants with reduced propensity to catalyze this Apelin-13 hydrolysis.

Yeast surface display [16,17] allows one to express active enzymes on the yeast surface (Supplementary Figure 1) and subsequently transfer these enzymes into contaminant-free ACE2 hydrolysis reaction buffer by simple centrifugation and resuspension. Combining this enzyme display technology with high performance liquid chromatography (LC) analysis of ACE2-mediated hydrolysis of authentic peptide substrates, e.g., Ang-II and Apelin-13, provides an efficient means of screening ACE2 mutant libraries to identify ACE2 variants with enhanced Ang-II hydrolysis and specificity profiles. Examination of an ACE2-small molecule inhibitor co-crystal structure and sequence alignment against structurally similar peptidases allows one to identify ACE2 amino acid residues that are likely to both play roles in substrate hydrolysis and be tolerant to substitutions [18]. Site-directed, e.g., NNB codon [19], ACE2 mutant libraries containing mutations at these residue positions are readily constructed and subsequently screened to identify improved variants using the above LC method.

In this work we use a yeast display-LC screening methodology to screen site-directed ACE2 mutant libraries and identify ACE2 mutants possessing both improved specificity toward Ang-II relative to Apelin-13 and Ang-II hydrolytic activity greater than or equal to that of wild type ACE2. These enhanced properties were observed for the ACE2 mutants regardless of whether evaluated in yeast-displayed or soluble, purified formats. The outcomes presented here can have an important impact in achieving broad deployment of ACE2-based approaches for prevention and treatment of a range of health conditions spanning both clinical applications in which ACE2 is currently being pursued and contexts in which the potential of ACE2 protein drugs is unexplored.

## Results

*Yeast surface display-based directed evolution of ACE2 for enhanced activity and specificity*

A *Saccharomyces cerevisiae* codon-optimized gene encoding the human ACE2 peptidase domain, amino acids 18-615, was well-expressed on the yeast cell surface (Supplementary Figure 2). LC analysis of reaction supernatants for ACE2-displaying yeast incubated with respective Ang-II and Apelin-13 peptides showed that yeast suspended in ACE2 reaction buffer hydrolyze more than 95% of these peptide substrates during a 2.5-hour room temperature reaction (Figure 2). ACE2-displaying yeast did not hydrolyze the Ang-I peptide; this outcome was expected given that the ACE2 hydrolysis $k_{cat}/K_m$ value for Ang-I is nearly 1,000-fold lower than those for Apelin-13 and Ang-II [10]. Given that Ang-I, Ang-II and Apelin-13 are all present in both blood and tissues *in vivo* we developed a multiplex substrate hydrolysis assay for ACE2 mutant library screening. Surprisingly, Ang-I acted as an inhibitor of ACE2-mediated Ang-II and Apelin-13 hydrolysis under these multiplex reaction conditions as respective conversions of Ang-II and Apelin-13 were reduced approximately five-fold relative to single substrate hydrolysis reactions (Figure 2).

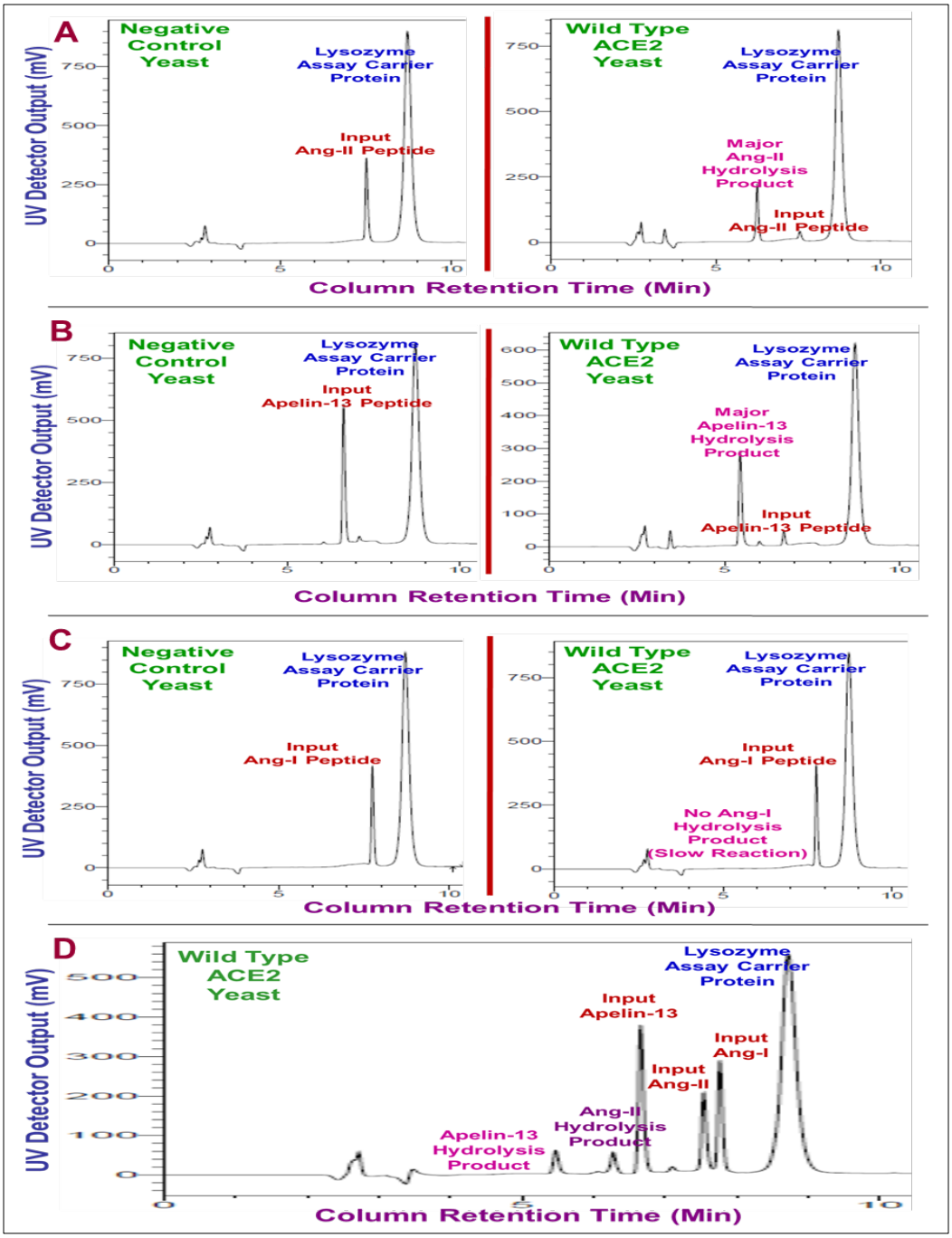


**Figure 2.** LC chromatograms for ACE2-displaying and negative control yeast incubated with ACE2 peptide substrates. Y-axes denote UV detector signal (mV at 214 nm). X-axes denote peptide elution time; input substrate and hydrolysis products denoted on figures. All reactions were carried out with $3*10^5$ yeast in 400 µL reaction volume with tumbling for 2.5 hours at room temperature. Horseradish peroxidase-displaying yeast (left panels) used as negative control. A) Reaction with 25 µM Ang-II. B) Reaction with 50 µM Apelin-13. C) Reaction with 25 µM Ang-I. D) Multiplex reaction containing 25 µM Ang-II, 50 µM Apelin-13 and 25 µM Ang-I. Lysozyme, added as carrier protein, appears in all chromatograms at elution time of 8.8 minutes.

Guided by the crystal structure of ACE2 [20] and observation of ACE2 active site residues conserved across structurally similar carboxypeptidases [18,20], where positions at which variation across homologues was observed were given preference over conserved positions, we created ten site-directed single mutant ACE2 libraries by introducing NNB (N denotes all four nucleotides while B denotes C, G or T) codons at ACE2 residues E145, N149, R273, T347, M360, K363, T371, F504, Y510 and R514 (Figure 3). Between five and fifteen clones for each site-directed ACE2 library were screened in substrate multiplex assays that contained 25 μM Ang-I, 25 μM Ang-II and 25 μM Apelin-13; these substrate concentrations provide broad LC signal dynamic range (Figure 2) and considerable margin for increases and decreases in Ang-II and Apelin-13 hydrolysis relative to wild type ACE2-displaying yeast.

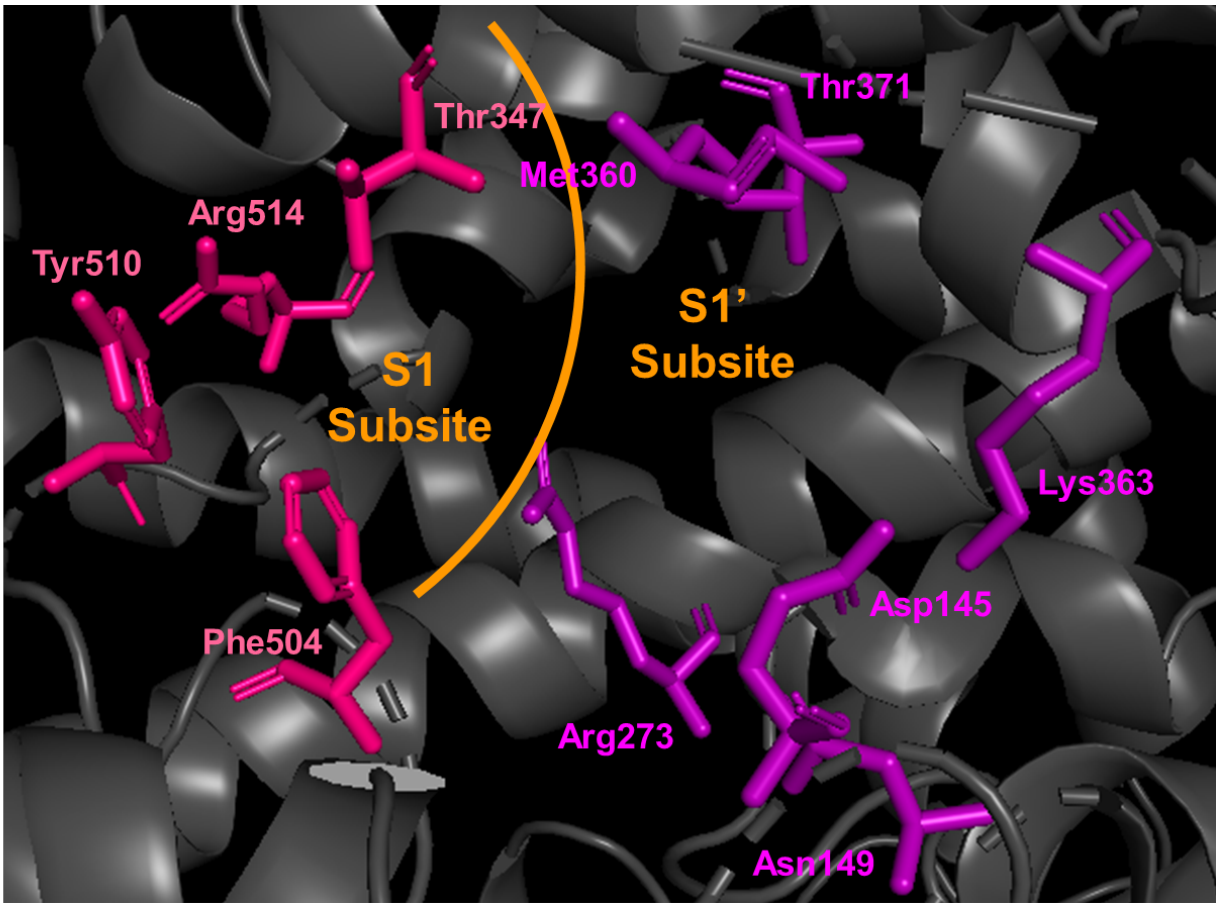


**Figure 3.** ACE2 active site residues chosen for site-directed single mutant library construction mapped onto ACE2 crystal structure (pdb entry 1R4L). For ACE2-mediated hydrolysis of the Ang-II octapeptide the ACE2 upstream S1 subsite (magenta residues) encases Ang-II Pro7 while the downstream S1' subsite (purple residues) accommodates Ang-II Phe8. Selected ACE2 residues and catalytic $Zn^{2+}$ ion hidden from image to provide enhanced view of ACE2 substrate-binding subsites. Figure created using Pymol.

More than half of the sampled clones from the R273, T347, F504 and R514 site-directed mutant libraries had hydrolytic activity toward Ang-II that was less than fifty percent of the wild type ACE2 activity (Supplementary Table 1) while the majority of assayed clones from the E145, N149 and K363 libraries possessed substrate hydrolysis profiles very similar to wild type ACE2. The M360, T371 and Y510 mutant libraries all contained multiple clones with substrate hydrolysis profiles,

i.e., absolute hydrolysis of Ang-II and Ang-II:Apelin-13 hydrolysis ratio, that were improved relative to wild type with the improvements being particularly large for two clones from each of these libraries (Figure 4).

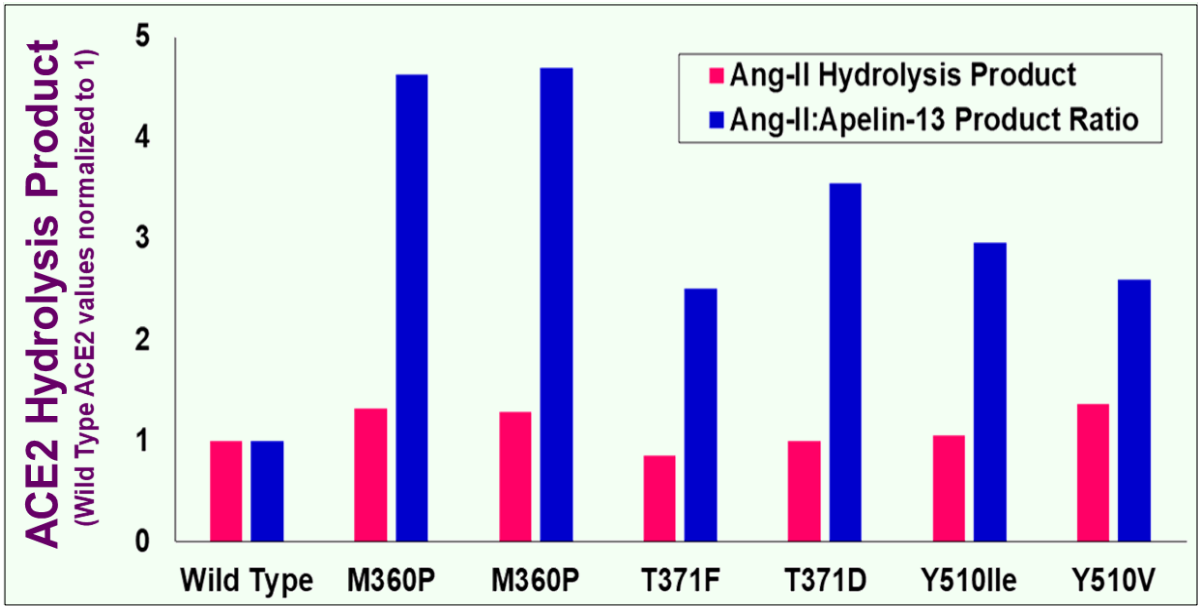


**Figure 4.** Substrate hydrolysis profiles for wild type and leading ACE2 single variants from position 360, 371 and 510 site-directed mutant libraries as observed in multiplex hydrolysis assays executed with 25 μM each Ang-I, Ang-II and Apelin-13. Y-axis values denote Ang-II hydrolysis product and ratio of Ang-II:Apelin-13 hydrolysis products for ACE2 variants relative to wild type; wild type values normalized to one. Ang-II and Apelin-13 hydrolysis products quantified by LC chromatogram peak integration (UV detector mV*sec). Hydrolysis of Ang-I was not detectable under these assay conditions. Both sequenced clones from the position 360 library carried Met to Pro mutations.

The M360P, T371D and Y510Ile mutants were used as parents in constructing six ACE2 double mutant libraries: M360P with NNB codon at position 371, M360P with NNB at position 510, T371D with NNB at 360, T371D with NNB at 510, Y510Ile with NNB at 360 and Y510Ile with NNB at 371. Five randomly sampled clones from each library were evaluated in multiplex hydrolysis assays to estimate the fractions of functionally impaired and improved clones in each library. As shown in Supplementary Table 2, the M360P/NNB 371, Y510Ile/NNB360 and Y510Ile/NNB 371 double mutant libraries warranted further screening by virtue of containing high fractions of active clones. Screening between eighteen and twenty-five additional clones from these libraries and sequencing the most promising clones yielded the collection of five leading double mutants: M360P/T371A, M360P/T371S, M360P/Y510Ile, M360L/Y510Ile and T371L/Y510Ile with multiplex hydrolysis assay activity profiles shown in Figure 5 (next page).

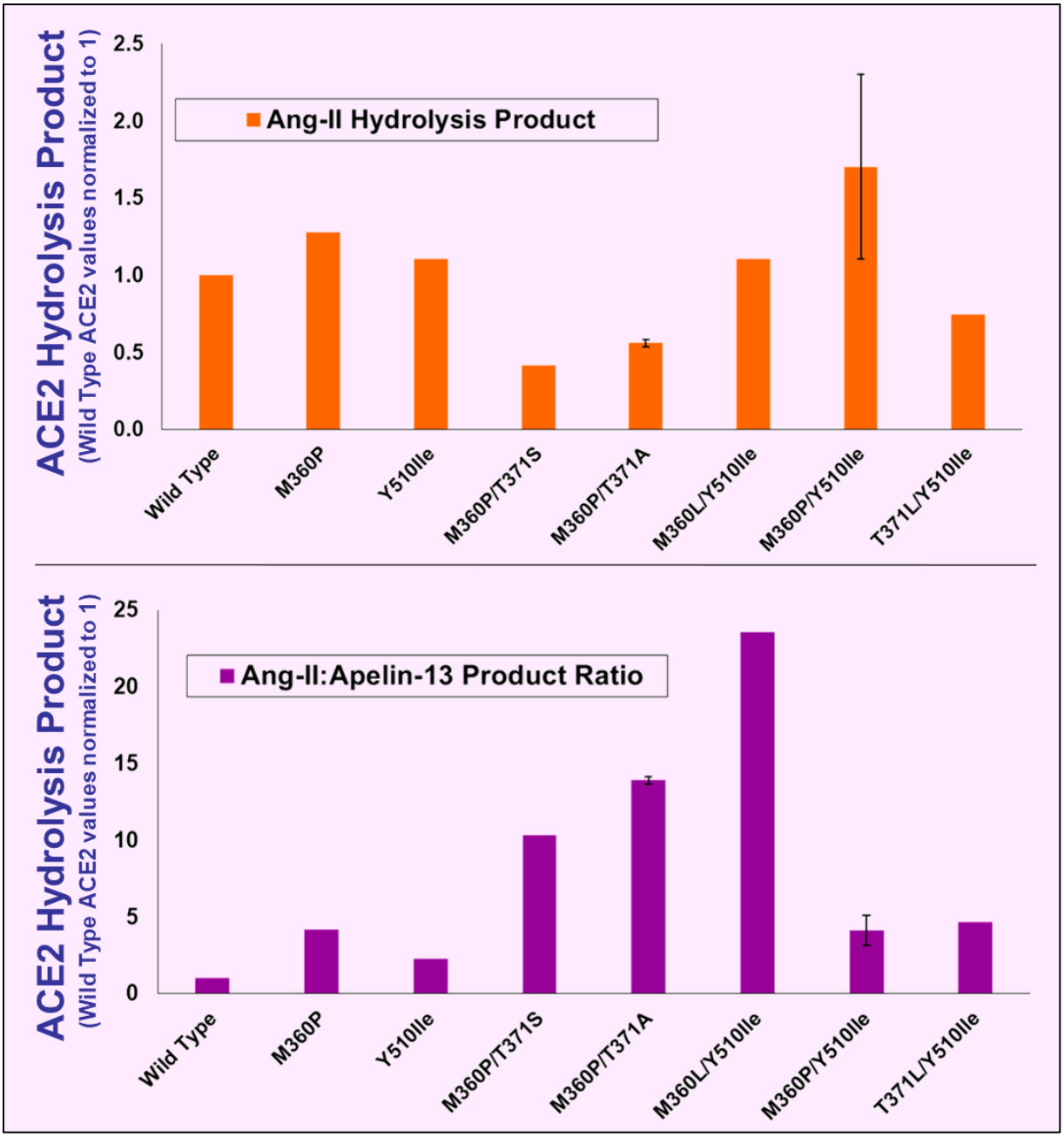


**Figure 5.** Substrate hydrolysis profiles for wild type ACE2, parental single variants and leading ACE2 variants identified in screening of 360-clone 7/NNB 371, 510-clone 11/NNB360 and 510-clone 11/NNB 371 double mutant libraries as observed in multiplex hydrolysis assays executed with 25 μM each Ang-I, Ang-II and Apelin-13. Y-axis values denote Ang-II hydrolysis product (upper panel) and ratio of Ang-II:Apelin-13 hydrolysis products (lower panel) for ACE2 variants relative to wild type; wild type values normalized to one. Ang-II and Apelin-13 hydrolysis products quantified by LC chromatogram peak integration (UV detector mV*sec). Hydrolysis of Ang-I was not detectable under these assay conditions. Error bars denote standard deviations for two assays for cases in which ACE2 variant sequencing showed that replicates of a given double mutant clone had been assayed during screening.

Given that our goal for this initial ACE2 activity modification effort was to demonstrate the ability to evolve improved ACE2 variants, as opposed to isolate the best possible variant from the ACE2 mutant libraries that were screened, we proceeded with soluble expression and purification of these five leading double mutants regardless of the number of mutant library clones screened having been below that required to achieve complete library coverage [19].

*Engineered ACE2s display enhanced kinetic properties*

Three of the leading double mutants, where difficulties were encountered in building the M360P/T371S construct, as well as the M360P and Y510Ile single mutants were cloned into a soluble secretion vector [21] and the ACE2 proteins expressed in Human Embryonic Kidney (HEK) cells. As shown in the SDS-PAGE gel of Supplementary Figure 3, greater than 90% pure protein was obtained for both wild type and mutant ACE2s. Post-purification yields were approximately 1 mg/L HEK culture supernatant.

Evaluation of ACE2 variant activity toward Ang-II and Apelin-13 in single substrate hydrolysis assays revealed that the M360P and M360P/Y510Ile mutants had hydrolytic activity less than ten percent of wild type on an equimolar basis. The other three ACE2 mutants: Y510Ile, M360L/Y510Ile and T371L/Y510Ile were evaluated, along with wild type ACE2, in single substrate initial rates experiments to determine kinetic parameters, i.e., $k_{cat}$ and $K_m$, for hydrolysis of Ang-II and Apelin-13.

As shown in Figure 6 (next page), all of the mutants hydrolyze Ang-II at rates ~ 50% or greater than those for wild type ACE2 at the lowest, and thus most physiologically relevant given levels of Ang-II found in blood (50-200 pM) [13,14] and tissues (200-300 pM) [15,22], ACE2 concentrations evaluated, i.e., 0.25 and 0.5 μM. Mutant catalytic rates become greater than those for wild type ACE2 as Ang-II concentration rises above 0.5 μM. These observations are reflected in the kinetic parameter values of Table 1; $k_{cat}$ values for ACE2 mutants are increased up to seven-fold relative to wild type while $K_m$ values are between five- and nine-fold greater than wild type.

**Table 1.** Ang-II and Apelin-13 hydrolysis kinetic parameters for wild type and mutant ACE2s. Parameter estimates obtained by using GraphPad Prism software to fit initial rates data that appears in Figure 6.

| ACE2 | Wild Type | Y510Ile | M360L/Y510Ile | T371L/Y510Ile |
|---|---|---|---|---|
| **Ang-II $k_{cat}$ ($s^{-1}$)** | 2.1 +/- 0.2 | 13.2 +/- 0.7 | 8.4 +/- 0.1 | 15.3 +/- 0.3 |
| **Ang-II $K_m$ (μM)** | 7.2 +/- 2.8 | 60.4 +/- 10.7 | 35.9 +/- 2.1 | 42.1 +/- 2.5 |
| **Ang-II $k_{cat}/K_m$ ($s^{-1}*M^{-1}$)** | $2.9*10^5$ | $2.2*10^5$ | $2.3*10^5$ | $3.6*10^5$ |
| **Apelin-13 $k_{cat}$ ($s^{-1}$)** | 10.3 +/- 1.2 | 23.1 +/- 0.6 | 10.4 +/- 0.3 | 8.6 +/- 0.3 |
| **Apelin-13 $K_m$ (μM)** | 25 +/- 10 | 330 +/- 20 | 200 +/- 12 | 130 +/- 15 |
| **Apelin-13 $k_{cat}/K_m$ ($s^{-1}*M^{-1}$)** | $4.1*10^5$ | $7.0*10^4$ | $5.2*10^4$ | $6.7*10^4$ |

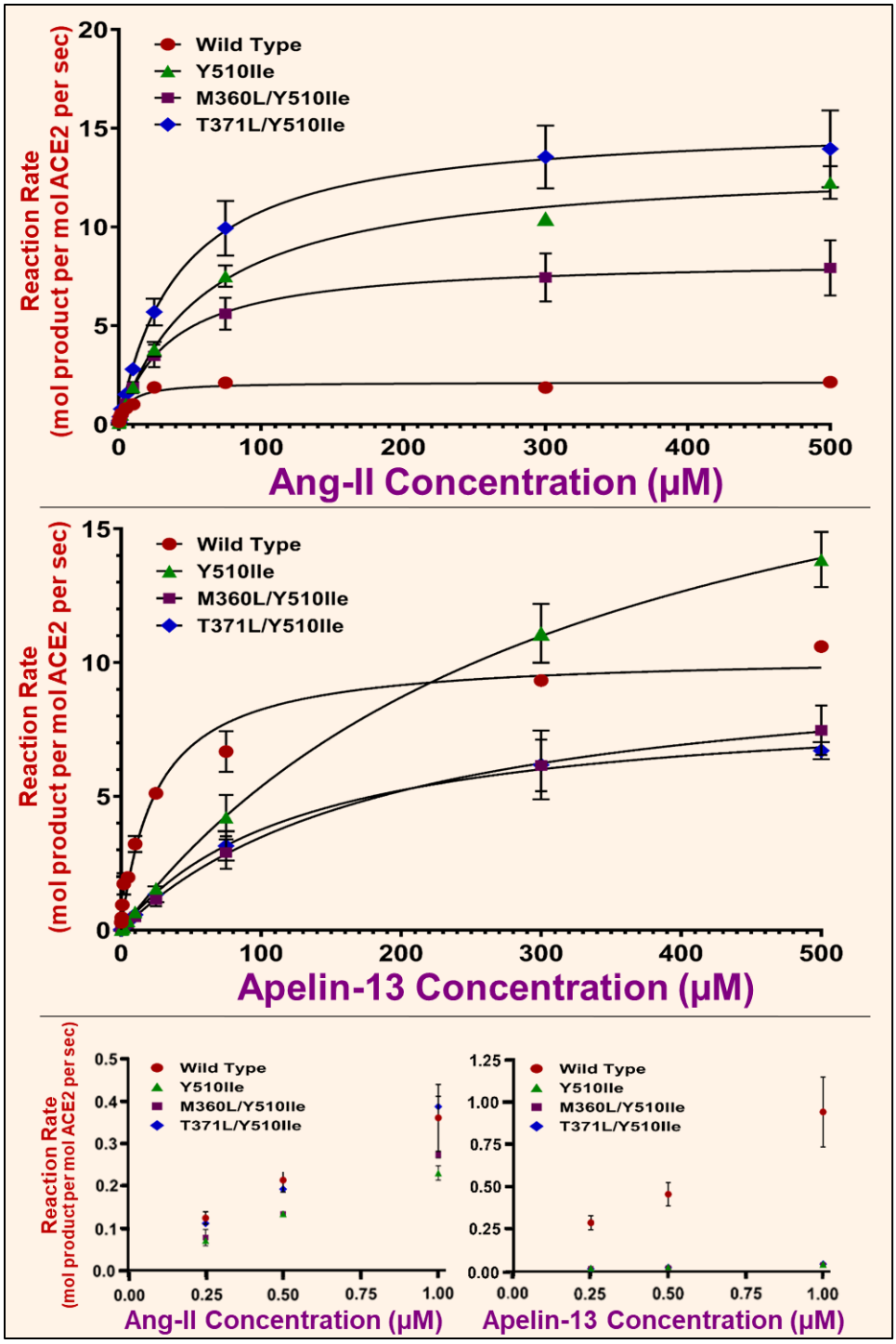


**Figure 6.** Initial rates plots for single substrate hydrolysis assays with respective Ang-II (upper panel) and Apelin-13 (middle panel) peptides. Assays contained 700 pM (Ang-II) or 1.4 nM (Apelin-13) ACE2 protein. Error bars denote standard deviations for duplicate assays; absence of error bars for some data points indicates standard deviation less than height of data point marker. Lines denote nonlinear regression data fits as calculated by GraphPad Prism software. Lower panel plots contain rate data for lowest three substrate peptide (0.25 μM, 0.5 μM and 1 μM) concentrations assayed in upper and middle panel.

The Apelin-13 initial rates data of Figure 6 shows that all mutants have less activity toward this substrate than does wild type ACE2. For sub-micromolar concentrations of this off-target substrate, which is found in blood at concentrations in the single-digit nM range [23], activity relative to wild type ACE2 is reduced between five- and ten-fold for all three mutants. Although the activity difference narrows with increasing Apelin-13 concentration, even at 500 μM substrate the Y510Ile single mutant is the only ACE2 variant hydrolyzing Apelin-13 at a rate matching or exceeding that for wild type ACE2. The mutant ACE2 Apelin-13 $K_m$ values of Table 1, which are between five and thirteen times that for wild type, illustrate the above described Apelin-13 hydrolysis behavior.

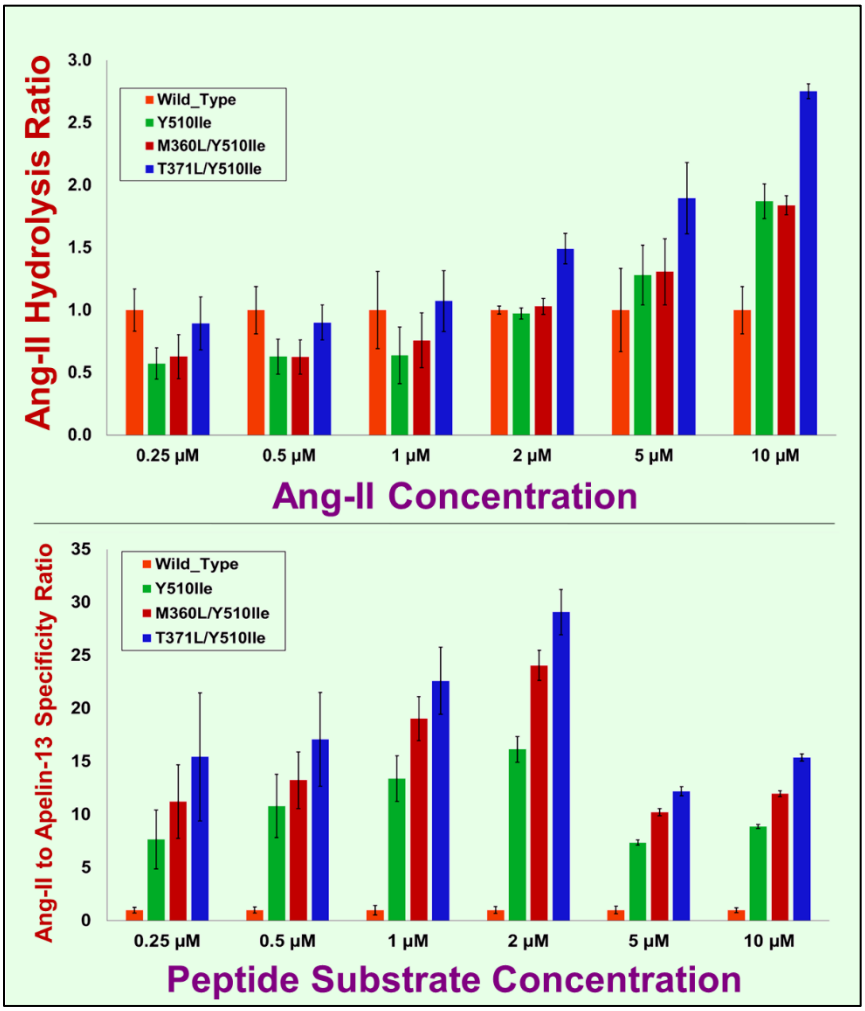


**Figure 7.** Comparison of mutant and wild type ACE2 Ang-II and Apelin-13 single substrate assay initial hydrolysis rates over the 0.25 μM to 10 μM peptide substrate range. Ratios are based on rate values presented in Figure 6 and are set to one for wild type ACE2. Ang-II hydrolysis ratio (upper panel) defined as mutant ACE2 hydrolysis rate divided by wild type ACE2 hydrolysis rate at a given Ang-II concentration. Ang-II to Apelin-13 specificity ratio (lower panel) defined as a mutant's Ang-II hydrolysis ratio for a given Ang-II concentration multiplied by the wild type ACE2 Apelin-13 hydrolysis rate and divided by that mutant's Apelin-13 hydrolysis rate with both of these rates having been measured at an Apelin-13 concentration matching that for the Ang-II hydrolysis ratio. Error bars reflect standard deviations for duplicate measurements and are determined using error propagation as described in Materials and Methods.

The bar plot of Figure 7 (preceding page) incorporates the single substrate hydrolysis assay results of Figure 6 in showing that all mutant ACE2s have Ang-II:Apelin-13 hydrolysis ratios greater than wild type regardless of substrate concentration. The T371L/Y510Ile double mutant is especially noteworthy in that it possesses both Ang-II hydrolysis rates equal to or greater than wild type and Ang-II:Apelin-13 hydrolytic activity ratios that are increased greater than ten-fold relative to wild type for all substrate concentrations assayed in initial rates studies.

To further compare the Ang-II and Apelin-13 hydrolysis profiles for the wild type and mutant ACE2s, multiplex peptide substrate hydrolysis assays were carried out. Two sets of assays with different, i.e., 700 pM and 250 pM, ACE2 concentrations were performed to assess whether ACE2 concentration impacts relative hydrolytic activity and specificity for the mutant and wild type enzymes. Regardless of substrate or ACE2 protein concentration, the mutant ACE2s hydrolyze at least half as much Ang-II as does the wild type enzyme (Figure 8) while Ang-II:Apelin-13 hydrolysis ratios are elevated at least three-fold for all mutant ACE2s across all reaction conditions. The leading ACE2 mutant identified in single substrate assays, i.e., T371L/Y510Ile, has Ang-II hydrolysis activity equal to or greater than wild type in all of the multiplex hydrolysis reactions and a five-fold or greater increase in specificity ratio for the majority of the multiplex reaction conditions.

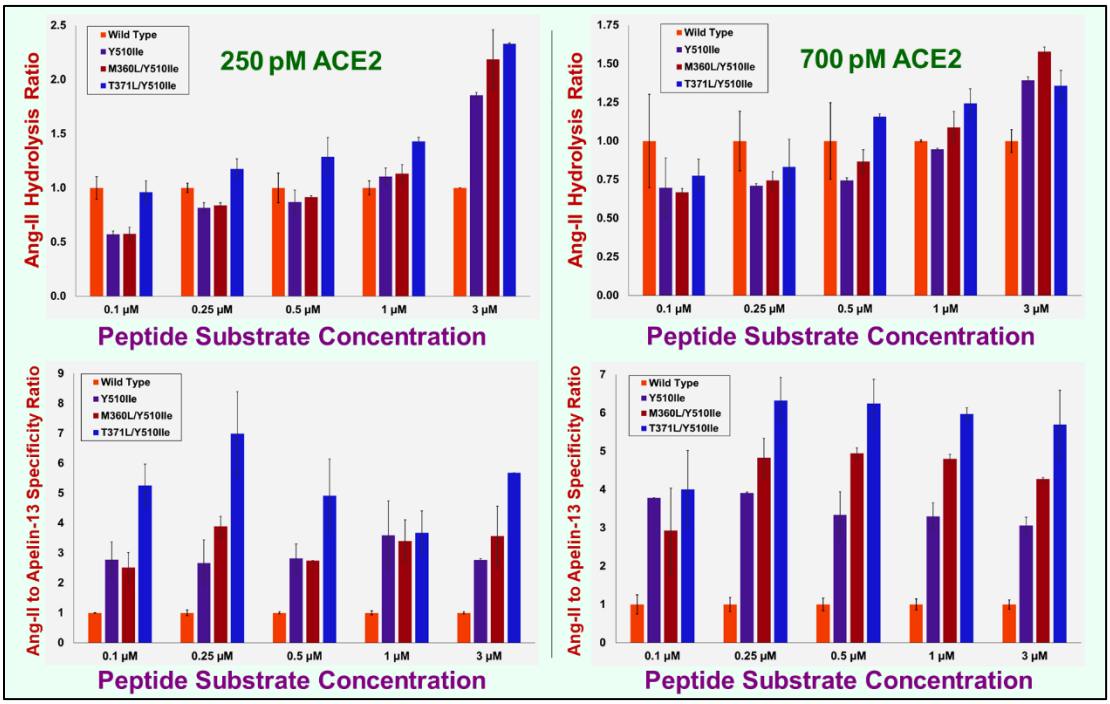


**Figure 8.** Mutant ACE2 Ang-II hydrolysis ratios and Ang-II specificity ratios for multiplex peptide substrate hydrolysis rate assays. Ratios are set to one for wild type ACE2. Ang-II hydrolysis ratio (upper panels) defined as mutant ACE2 hydrolysis rate divided by wild type ACE2 hydrolysis rate at a given substrate concentration. Ang-II to Apelin-13 specificity ratio (lower panels) defined as a mutant's Ang-II hydrolysis ratio for a given Ang-II concentration multiplied by the wild type ACE2 Apelin-13 hydrolysis rate and divided by that mutant's Apelin-13 hydrolysis rate. Ang-I, Ang-II and Apelin-13 were present at identical concentrations in each reaction. Left panels depict results for 250 pM ACE2 reaction condition, right panels show results for 700 pM ACE2. Error bars denote standard deviations for duplicate measurements.

Supplementary Figure 4 compares the Ang-II and Apelin-13 hydrolysis rates across single and multiplex substrate hydrolysis assays for the lowest substrate concentration, i.e., 0.25 μM, at which data was obtained for both single and multiplex assay formats. The presence of multiple substrates reduces hydrolysis rates for both Ang-II and Apelin-13. Ang-II hydrolysis rates are reduced between two- and three-fold while Apelin-13 hydrolysis rates are reduced by factors ranging from three to nine. Given the results presented in Figure 2, which indicate that Ang-I inhibits ACE2 hydrolysis of Ang-II and Apelin-13, it appears likely that the presence of Ang-I in the multiplex reactions is a substantial contributor to the observed reduction in Ang-II and Apelin-13 hydrolysis rates.

Examination of the crystal structure of ACE2 complexed with a small molecule inhibitor [21,24] allows postulation of mechanisms by which the M360L, T371L and Y510Ile mutations influence ACE2's hydrolytic activity and specificity. Y510 resides in the S1 subsite of ACE2's substrate binding pocket (Figure 9). ACE2 substrates [24], with the exception of the slowly-hydrolyzed Ang-I peptide, feature residues with small sidechains, i.e., Pro or Leu, at the P1 position; both Ang-II and Apelin-13 carry Pro at this position. Changing Tyr to Ile may increase Ang-II hydrolysis by enlarging the S1 subsite and/or creating favorable hydrophobic interactions between ACE2 and the Ang-II Pro sidechain.

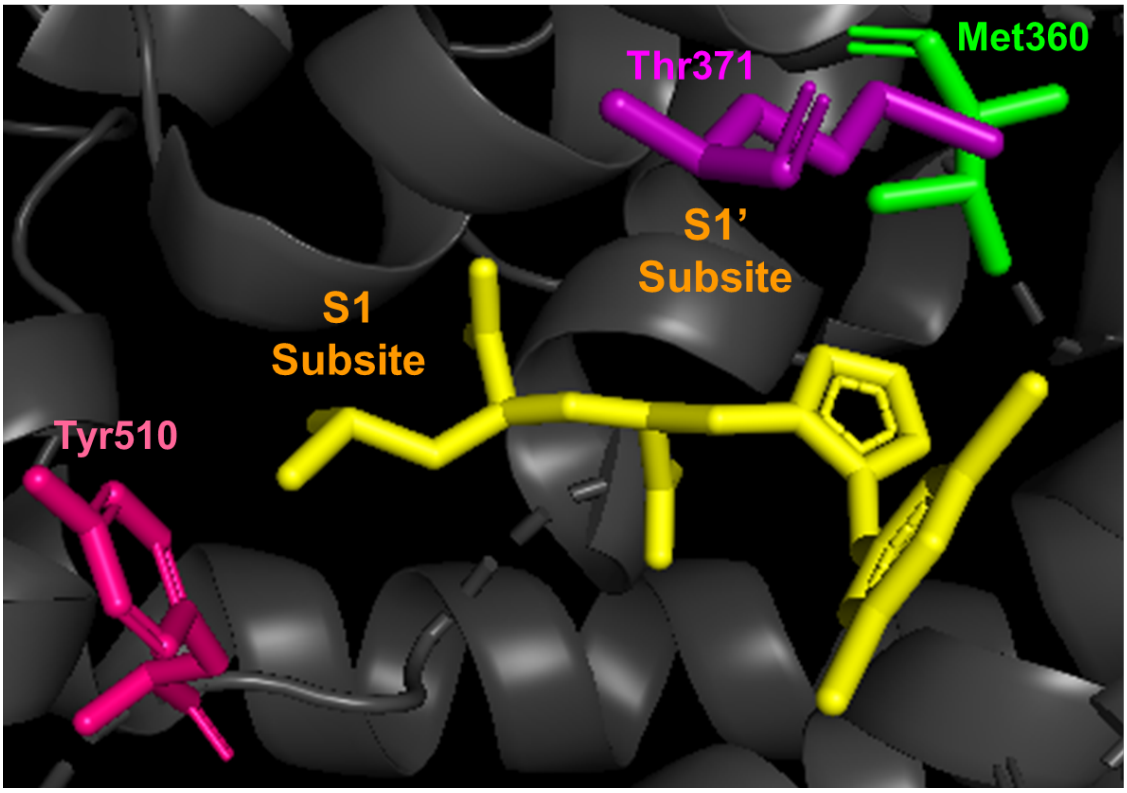


**Figure 9.** Positioning of key residues Met360 (green), Thr371 (purple) and Tyr510 (magenta) in ACE2 substrate binding pocket (pdb entry 1R4L). Co-crystallized ACE2 small molecule inhibitor denoted in yellow. Orange arc denotes approximate boundary between upstream S1 subsite and downstream S1' subsite. Selected ACE2 residues and catalytic $Zn^{2+}$ ion hidden from image to provide enhanced view of M360, T371 and Y510 ACE2 residues and small molecule inhibitor. Figure created using Pymol.

The increase in Ang-II specificity arising from Y510Ile mutation may be the result of differences in interactions between the respective wild type and mutant ACE2s and the substrate at upstream substrate residue positions, where all of these upstream amino acids differ across Ang-II and Apelin-13, affecting the way in which the substrate Pro is oriented within ACE2's S1 subsite.

The sidechains of M360 and T371 line the interior of ACE2's S1' subsite. This subsite accommodates the C-terminal Phe of both Ang-II and Apelin-13. The similarity in sidechain size among Met, Leu and Thr suggests that hydrophobic effects contribute to the observed impacts of the M360L and T371L substitutions on Ang-II hydrolysis rate and specificity toward Ang-II relative to Apelin-13. Given that Ang-II and Apelin-13 are identical at the P1' position, it is possible that substrate positioning within ACE2's binding pocket, and thus substrate hydrolysis rate and the concentration dependence thereof, is affected by enzyme-substrate interactions that occur between ACE2 residues and substrate amino acids upstream of the P1' position. As alluded to above, such interactions are likely to be distinct across the Ang-II and Apelin-13 peptides and thus could cause mutations in the ACE2 substrate binding pocket, e.g., M360L and T371L, to have different effects on ACE2 activity toward these respective substrates.

*Engineered ACE2s retain specificity against other off-target substrates*

Characterizing mutant ACE2 activity toward off-target peptides, other than Apelin-13, known to be hydrolyzed by wild type ACE2 *in vivo* enlightens whether our directed evolution method may feature the caveat of identifying promiscuous mutants that could possess increased propensity to cause undesirable side effects when administered as therapeutics. Initial rates data for wild type and mutant ACE2 hydrolysis of Ang-I (Figure 10 - next page) shows that the T371L/Y510Ile mutant, which has the most desirable activity profile in terms of Ang-II and Apelin-13 hydrolysis, hydrolyzes Ang-I at rates that are statistically identical to wild type.

This outcome suggests that our ACE2 directed evolution method can identify variants that are both improved with respect to Ang-II and Apelin-13 hydrolysis profiles and free of increased activity toward other ACE2 substrates. Also noteworthy is that the wild type and mutant ACE2s have Ang-I hydrolysis rates that are reduced at least 100-fold relative to those measured for identical concentrations of Ang-II over the entire assay range (Supplementary Table 3). This outcome is in accord with the published observation that the Ang-I hydrolysis $k_{cat}$ value for wild type ACE2 is approximately one-hundred times less than that for hydrolysis of Ang-II [10].

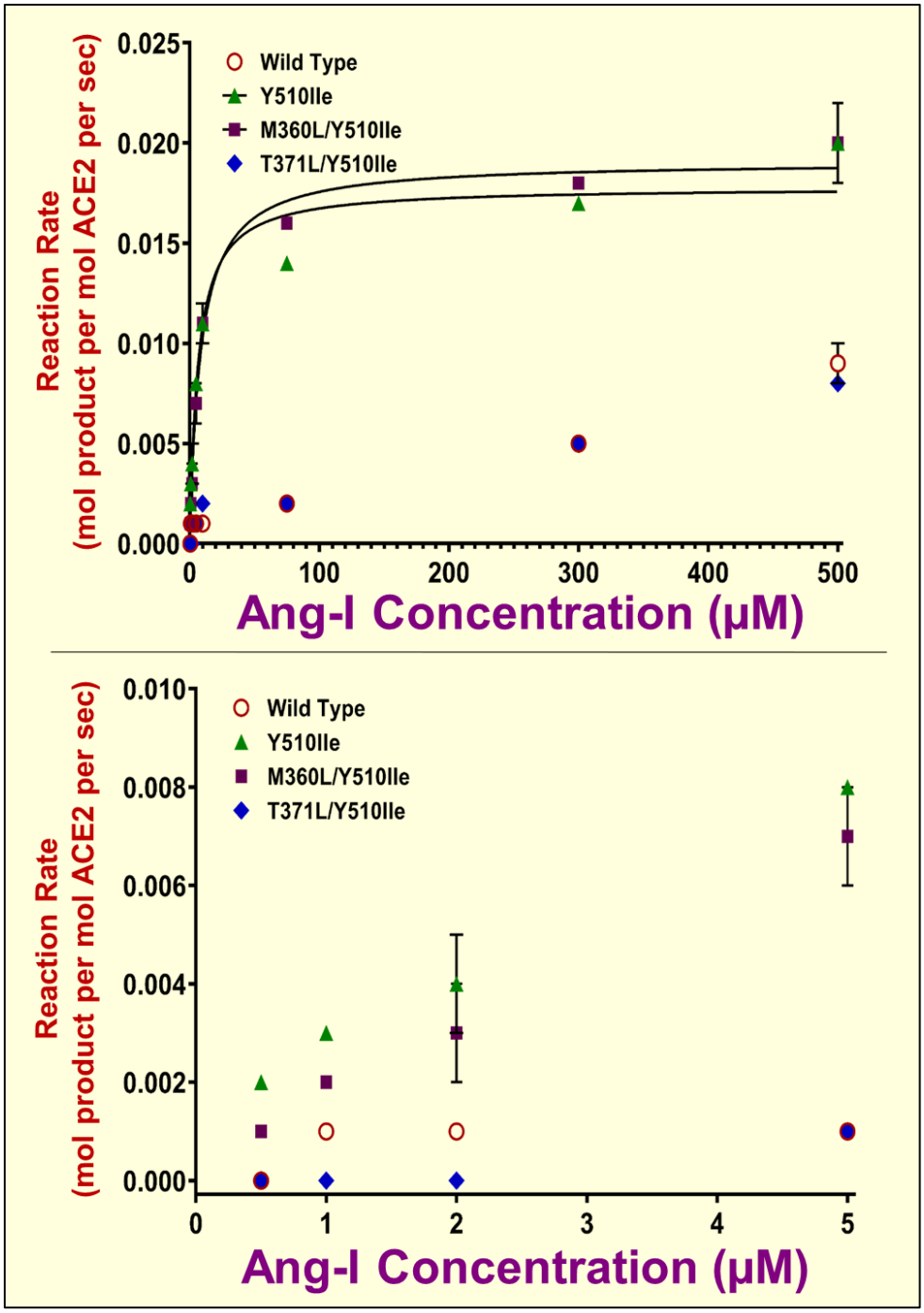


**Figure 10.** Initial rates plots for single substrate Ang-I hydrolysis assays. Assays contained 1.75 nM ACE2 protein. Error bars denote standard deviations for duplicate assays; absence of error bars for some data points indicates standard deviation less than height of data point marker. Lines denote nonlinear regression data fits as calculated by GraphPad Prism software. Highest Ang-I concentration assayed, i.e., 500 μM, was below that required to accurately estimate kinetic parameters for wild type and T371L/M510Ile ACE2s. Lower panel plot contains rate data for lowest four Ang-I (0.5 μM, 1 μM, 2 μM and 5 μM) concentrations assayed in upper panel.

In further exploring whether ACE2 mutants possess increased activity toward off-target substrates hydrolysis assays featuring the Ang1-9 nonapeptide, DRVYIFPFH, which is not hydrolyzed by wild type ACE2 [10], were carried out. None of the mutant ACE2s exhibited activity toward this peptide as determined by LC analysis (Supplementary Figure 5). Additional evaluation of ACE2 variants specificity was performed by executing single substrate hydrolysis assays with the ACE2 natural substrate Des-Arg9-bradykinin (dR9-bk), an octapeptide with sequence RPPGFSPF [10,25]. The bar plots of Supplementary Figure 6 show that dR9-bk initial hydrolysis rates for all three mutants were equal to or less than wild type across all assayed substrate concentrations, i.e., 1 μM to 75 μM. Taken with the above observations of mutant ACE2 activities toward Ang-I and Ang1-9, these dR9-kb hydrolysis assay outcomes suggest that ACE2's activity profile with respect to Ang-II and Apelin-13 hydrolysis can be enhanced without concomitant compromise of specificity toward off-target substrates other than Apelin-13.

## Discussion

The clinical potential of our evolved ACE2 mutants could be further enhanced by reducing their $K_m$ values for Ang-II hydrolysis while concomitantly maintaining or increasing $k_{cat}$. Given that, as noted above, our goal for this work was demonstrating the utility of our method for evolving improved ACE2 variants rather than identifying the best possible variants given the ten ACE2 residues that were mutated, it is likely that an evolutionary process that begins with a more comprehensive screen of the existing ACE2 single site saturation mutant libraries would lead to isolation of ACE2 double mutants with activity and specificity profiles that are superior to those for the current leading, i.e., T371L/Y510Ile, double mutant.

Screening approximately ninety clones per site-directed single mutant library [19] is expected to correspond with a greater than 95% probability of identifying the best mutant in each library. Given our LC method's screening capacity of approximately fifty clones per day, ninety clones from all ten of the active site saturation mutant libraries could be screened in one month. Sequence information for the leading ACE2 single mutants could then be used to, as was done in this work, guide construction of double mutant libraries in which one mutation is fixed and a second amino acid position is varied by introduction of a NNB codon. In less than two months up to twenty such double mutant libraries could be screened at the above noted 95% coverage level. Given the much more expansive nature of both this envisioned double mutant library screen and the underlying single mutant library evaluation relative to what has been carried out previously, it appears nearly certain that pursuing this more comprehensive directed evolution strategy would uncover ACE2 mutants that are markedly augmented relative to the T371L/Y510Ile variant.

A comparison of the substrate specificity results presented in Supplementary Figure 7 underscores the value of evaluating ACE2 mutants in multiplex peptide substrate hydrolysis assays. In particular, the presence of multiple substrates reduces Ang-II:Apelin-13 hydrolysis ratios relative to those calculated based on hydrolysis rates for single substrate hydrolysis assays. This compression of substrate hydrolysis ratios indicates that in addition to being more representative of *in vivo* conditions than is the case for single substrate assays, multiplex

substrate assays provide a more stringent test of mutant ACE2 substrate specificity relative to the wild type enzyme.

Insight regarding the origin of this compression of specificity ratios can be gained by connecting two observations. First, in single peptide assays featuring substrate concentrations that fall within the range of substrate concentrations used in multiplex assays the ACE2 mutants hydrolyze Ang-II at rates that are between three- and ten-fold greater than those corresponding to hydrolysis of Apelin-13. Second, multiplex substrate conditions cause the ACE2 active site to be occupied by different peptides at different timepoints during the hydrolysis assay and thus Ang-I and Apelin-13 act as competitive inhibitors of Ang-II hydrolysis; Apelin-13 hydrolysis is similarly subject to competitive inhibition by Ang-I and Ang-II. During a multiplex hydrolysis reaction the time of ACE2 active site occupation by Ang-I or Apelin-13 is greater relative to the time required for an Ang-II hydrolysis event than is the time of active site occupation by Ang-I or Ang-II relative to the time required for an Apelin-13 hydrolysis event. This difference leads to a larger fractional reduction in the rate of Ang-II hydrolysis than in the rate of Apelin-13 hydrolysis and causes the observed decrease in Ang-II:Apelin-13 specificity ratios for multiplex relative to single substrate assays.

The large difference, with the soluble mutant proteins having less than 10% of soluble wild type ACE2 activity toward Ang-II and Apelin-13, in hydrolytic activity relative to wild type ACE2 for the M360P and M360P/Y510Ile mutants across yeast-displayed and soluble protein formats illustrates the need to consider sequence diversity when choosing variants for soluble expression following yeast-displayed ACE2 library screening; if all of the ACE2 variants chosen for soluble expression after double mutant library screening had carried the M360P mutation the desirable effects of the T371L and Y510Ile substitutions in the context of soluble ACE2s would have been masked by the markedly reduced activity associated with the M360P mutation. The low level of hydrolytic activity observed for soluble ACE2 variants carrying the M360P substitution is not without precedent as display on the yeast surface has been observed to stabilize active conformations of protein mutants that are prone to taking on inactive conformations when free in solution [26,27].

Our directed evolution method has enabled isolation of ACE2 variants with potential to outperform wild type ACE2 as protein therapeutics. This outcome can be important in advancing current ACE2 therapeutic initiatives, such as treating respiratory distress associated with traumatic injuries or viral infection [4], and giving rise to new ACE2 biomedical applications including Alzheimer's Disease therapy [7] and employing peptidase-peptide orthogonal pairs [28,29] to enable localized prodrug activation. Furthermore, these results provide a foundation for developing additional directed evolution methods, such as microfluidics droplet-based screening to augment ACE2 activity and specificity [30], that facilitate sampling larger swaths of ACE2 sequence space and thus further enable ACE2 to realize its potential as an agent for treating and preventing a wide range of health conditions.

## Materials and Methods

*ACE2 library generation and screening*

Residues 18-615 of the human (UniProt Q9BYF1) ACE2 genes were synthesized as a yeast codon-optimized gBlock (Integrated DNA Technologies, Coralville, IA) and ligated into the NheI and MluI sites of yeast display vector VLRB.2D-aga2 (provided by Dane Wittrup, MIT); this vector fuses the aga2 protein to the C-terminus of ACE2 (Supplementary Figure 1). Site-directed mutant libraries were constructed via overlap extension PCR and standard ligation using T4 DNA ligase (New England Biolabs, Beverly, MA). Oligonucleotide primers carrying NNB base triplets were purchased from Integrated DNA Technologies. The degenerate 'B' base is comprised of a mixture of C, G and T bases while the degenerate 'N' base is composed of all four nucleotide bases. Primers CDspLt (5'-GTCTTGTTGGCTATCTTCGCTG-3') and CDspRt (5'-GTCGTTGACAAAGAGTACG-3') were used as outer primers for ACE2 gene amplification reactions. Overlap extension PCR products were digested using NheI and MluI (New England Biolabs) and ligated into the yeast surface display vector VLRB.2D-aga2 digested with these same two enzymes. Overnight ligation reactions were desalted using a DNA Clean & Concentrate-5 column (Zymo Research, Orange, CA) and transformed into chemically competent NEB 5$\alpha$ cells (New England Biolabs).

For each transformation cells were plated onto three LB plates containing 100 $\mu$g/mL carbenicillin and after overnight incubation at 30°C all colonies on plates for each respective transformation were scraped into 10 mL of LB + carbenicillin liquid media and grown overnight at 30°C. Total colony counts for each single site-directed mutant library ranged from 500 to 2,000; numbers considerably greater than the fewer than 50 colonies observed for a negative control ligation reaction that contained digested VLRB.2D-aga2 backbone DNA absent any ACE2 gene insert.

DNA was harvested from overnight liquid cultures using the Qiagen Spin Miniprep Kit (Qiagen, Valencia, CA) and transformed into the EBY100 yeast surface display strain [16] that had been made chemically competent using the Frozen EZ-Yeast Transformation II Kit (Zymo Research). For each single site-directed mutant library transformed yeast were plated onto three each Synthetic Dropout minus Tryptophan (SD -Trp) plates and incubated at 30° C for two days. Individual yeast colonies were picked into 4mL of pH 4.5 Sabouraud Dextrose Casamino Acid media (SDCAA: Components per liter - 20 g dextrose, 6.7 grams yeast nitrogen base (VWR Scientific, Radnor, PA), 5 g Casamino Acids (VWR), 10.4 g sodium citrate, 7.4 g citric acid monohydrate) and grown overnight at 30°C and 250 rpm. For induction of ACE2 display a 5 mL pH 7.4 Sabouraud Galactose Casamino Acid (SGCAA: Components per liter - 8.6 g $NaH_2PO*H_2O$, 5.4 g $Na_2HPO_4$, 20 g galactose, 6.7 g yeast nitrogen base, 5 g Casamino Acids) culture was started at an optical density, as measured at 600 nm, of 0.5 and shaken overnight at 250 rpm and 20°C.

For LC determination of yeast-displayed ACE2 peptidase activity 35 µL of induced yeast culture was transferred to 500 µL of pH 7.4 Phosphate Buffered Saline (PBS) containing 0.1% (wt/vol) bovine serum albumin (BSA) and centrifuged at 4000g for one minute. Yeast were resuspended

in 400 µL of ACE2 reaction buffer (50 mM 2-(N-morpholino)ethanesulfonic acid (MES), 300 mM NaCl, 10 µM $ZnCl_2$, 0.02% w/v Hen Egg Lysozyme (Sigma-Aldrich, St. Louis, MO) as carrier protein, pH 6.5) containing 25 µM each Angiotensin-I (Anaspec, Fremont, CA), Angiotensin-II (Anaspec) and Apelin-13 (Bachem, Torrance, CA) and tumbled in microfuge tubes at 20 rpm at room temperature for 2.5 hours. Reactions were centrifuged at 9000g for one minute to pellet yeast and supernatants withdrawn for LC analysis.

Liquid chromatography (LC) analyses were performed on a Shimadzu 2020 LC-MS apparatus operating in UV detection mode at 214 nm. Sixty-five µL of ACE2 reaction were injected onto a 3x150 mm, 100 Å, 5 *u*m Polar C18 Luna Omega column (Phenomenex, Torrance, CA) using a linear gradient of 11% B to 100% B over 25 minutes with 5 minutes at final conditions and 8-minute re-equilibration. Mobile phase A consisted of 0.02% (v/v) trifluoroacetic acid in water, and mobile phase B consisted of 0.016% (v/v) trifluoroacetic acid in acetonitrile. Mobile phase flowrate was maintained at 0.3 mL/min throughout sample analysis. Hydrolysis product peaks were identified by comparison with chromatograms for reactions carried out using yeast displaying a negative control protein (horseradish peroxidase) and the area under the LC chromatogram curve, i.e, UV detector millivolts multiplied by elution timespan in seconds, was used as the metric for amount of product formed during the hydrolysis reaction.

For construction of ACE2 double mutant libraries that used leading single mutant clones, i.e., clone 360-7, 371-11, and 510-11 as described in the Results section, plasmids were rescued from 1 mL of yeast liquid culture using the Zymo Research Yeast Plasmid Miniprep II Kit. Rescued plasmids were used as templates for overlap PCR reactions carried out to introduce NNB codons, at the positions noted in the Results section, into the three respective single mutant ACE2 parent genes. Digestion and ligation of double mutant library PCR product DNA, *E. coli* transformation, *E. coli* culturing, double mutant library plasmid harvesting and EBY100 yeast transformations were carried out using procedures, as described above, identical to those for site-directed ACE2 single mutant libraries. Sequences for leading ACE2 double mutants were obtained by using the Zymo Yeast Plasmid Miniprep II kit, amplifying double mutant ACE2 genes using primers CDspLt and CDspRt, purifying the PCR products using a Zymo Clean & Concentrator-5 column and sequencing the PCR products using primers CDspLt, CDspRt and SqHmFw (5'-GGACTTTCAGGAAGACAACG-3').

*Soluble expression & purification of wild type and ACE2 variants*

Plasmid pcDNA3-sACE2(WT)-8his [21], which encodes human ACE2 residues 1-615 with native human codon representation and puts secretion of the gene product, with a C-terminal His8 tag, from mammalian cells under control of the cytomegalovirus CMV promoter, was used as template for creation of ACE2 genes carrying hydrolysis profile-modifying mutations identified during yeast displayed-ACE2 library screening. Mutant genes were constructed by overlap extension PCR using outer primers SqLtPck (5'-CGTGGATAGCGGTTTGACTCAC-3') and PckRvSq (5'-CCTACTCAGACAATGCGATGC-3'), digested NheI-BamHI (New England Biolabs) and ligated into pcDNA3-sACE2(WT)-8his that had been digested using these same enzymes. Overnight

ligation reactions were desalted, transformed into chemically competent NEB 5α cells as above and plated onto LB plates containing 100 μg/mL carbenicillin. Individual transformants were picked into 5 mL of LB media containing 100 μg/mL carbenicillin and incubated overnight at 37°C. DNA was harvested from overnight liquid cultures using the Qiagen Spin Miniprep Kit and inserted mutant ACE2 genes were verified by sequencing using primers SqLtPck, PckRvSq and PckF260 (5'-GTTACTGATGCAATGGTGGACC-3').

Human Embryonic Kidney 293T cells (Product #CRL-3216, ATCC, Manassas, VA) were grown in DMEM (ATCC) supplemented with 10% Fetal Bovine Serum (FBS), 2mM L-glutamate (Invitrogen, Carlsbad, CA), and 1x Penicillin-Streptomycin (Invitrogen) in 100 mm tissue culture treated dishes under a 5% $CO_2$ atmosphere at 37°C. Upon reaching ~ 70% confluence cells were transfected with 7 µg of ACE2 expression plasmid DNA and 10 µL of jetPRIME transfection reagent (PolyPlus, Illkirch-Graffenstaden, France) per the manufacturer's instructions. Two dishes of HEK cells were transfected for each ACE2 protein being expressed. Following the four-hour transfection interval DMEM containing DNA and transfection reagent was replaced with 10 mL of OptiMEM (Invitrogen) supplemented with 1x Pen-Strep and ACE2 expression was allowed to proceed for 40-48 hours at 37°C under 5% $CO_2$.

Media was withdrawn from culture dishes, pooled for duplicate transfections, and centrifuged at 500g for 5 minutes. Supernatants were syringe filtered using 0.22 µm polyethersulfone (PES) Whatman PuraDisc filters (Cytiva, Marlborough, MA). Supernatant concentration and buffer exchange into pH 7.4 PBS was performed using 30-kDa MWCO VivaSpin20 centrifugal concentrator units (Cytiva). $His_8$-tagged ACE2 proteins were purified from concentrated, buffer exchanged supernatants. Concentrated supernatants were brought to a final volume of 1 mL by addition of pH 7.4 PBS, adjusted to an imidazole concentration of 10 mM and tumbled head-over-head at 20 rpm in microfuge tubes with 25 μL of Qiagen Ni-NTA resin for 1 h at room temperature. Resin was subsequently washed with 1 mL PBS and 1 mL PBS/15 mM imidazole prior to ACE2 elution via 15-minute room temperature incubation of resin in 140 μL of pH7.4 PBS containing 250 mM imidazole. Eluted ACE2 proteins were buffer exchanged into 25mM Tris-HCl, pH 7.5 containing 10 µM $ZnCl_2$ using Zeba Spin desalting columns (Fisher Scientific, Waltham, MA) and protein concentrations determined using the Pierce Coomassie Protein Assay kit (Fisher Scientific).

SDS-PAGE analysis of purified ACE2s was carried out using a LIfeTech Mini Gel Tank electrophoresis system. Approximately 1 μg of purified, desalted ACE2 was loaded into each well of a Novex 4-20% Tris-Glycine gel and electrophoresis was performed at 200 volts for 45 minutes. PageRuler Unstained Protein Ladder (Fisher Scientific) was used as a molecular weight standard. Gels were stained with Simply Blue SafeStain (Invitrogen) following electrophoresis.

*Activity and specificity profiling of purified ACE2 proteins*

Peptide substrate hydrolysis assays were carried out at room temperature and 150 µL scale in 96-well plates using 50 mM MES, 300 mM NaCl, 10 µM $ZnCl_2$, 0.01% (vol/vol) Brij-35 (Sigma-

Aldrich) as reaction buffer. Reactions were halted by addition of 15 μL of 1M EDTA solution, pH 8, after intervals, which ranged from three minutes to 2.5 hours, during which less than 15% of the input peptide substrate had been hydrolyzed. ACE2 concentrations added to assays for the various peptide substrates evaluated were as follows: Ang-I/1.75 nM, Ang-II/700 pM, Apelin-13/1.4 nM, des-Arg9-bradykinin/700 pM, Ang (1-9)/700 pM, Multiplex/700 pM or 250 pM. Des-Arg9-bradykinin and Ang1-9 were purchased from Anaspec and ApexBio (Houston, TX) respectively.

Moles of product formed in hydrolysis reactions used for ACE2 activity and specificity profiling were determined by comparing area under the curve for LC chromatograms corresponding to these reactions to areas under the curve observed for control reactions in which > 95% input substrate conversion was achieved by incubation of substrate with 25 nM recombinant human ACE2 commercial standard (BioLegend, San Diego, CA) for between one and four hours pending peptide substrate. Elution times for peptide substrate inputs and hydrolysis products were determined by comparing chromatograms for the 25 nM ACE2 commercial standard reactions to input peptide reaction mixtures to which no ACE2 was added. LC analysis injection volumes and mobile phase gradient parameters were identical to those described above for yeast-displayed ACE2 library screening. Kinetic parameters for Ang-I, Ang-II and Apelin-13 hydrolysis were determined by fitting initial rates data using GraphPad Prism software (GraphPad, San Diego, CA). Standard deviations for ratios of hydrolysis rates that include values measured in single substrate hydrolysis assays were calculated by inserting the average of duplicate measurements and the standard deviation for that average into the equation -

$$For\ A = \frac{B}{C}$$

$$StDev\ A = A * \sqrt{\left(\frac{StDevB}{B}\right)^2 + \left(\frac{StDevC}{C}\right)^2}$$

For single substrate hydrolysis rate ratios B denotes mutant ACE2 hydrolysis rate and C denotes wild type ACE2 hydrolysis rate. For mutant ACE2:wild type Ang-II:Apelin-13 hydrolysis rate specificity ratios, B denotes mutant ACE2 Ang-II:Apelin-13 hydrolysis rate ratio and C denotes wild type ACE2 Ang-II:Apelin-13 hydrolysis rate ratio.

**Acknowledgements**

This work was supported by the US National Institutes of Health (5R35GM119854). "The content is solely the responsibility of the authors and does not necessarily represent the official views of the National Institutes of Health."

**References**

1. Marquez A, Wysocki J, Pandit J, Batlle D, An update on ACE2 amplification and its therapeutic potential. *Acta Physiol (Oxf).* Jan;231(1):e13513 (2021)

2. Shenoy V, Qi Y, Katovich MJ, Raizada MK, ACE2, a promising therapeutic target for pulmonary hypertension. *Curr Opin Pharmacol.* 11(2):150-5 (2011).

3. Hay M *et al.* A novel Angiotensin-(1-7) Glycosylated Mas Receptor Agonist for Treating Vascular Cognitive Impairment and Inflammation-Related Memory Dysfunction. *J Pharmacol Exp Ther.* 369(1):9-25 (2019).

4. Zoufaly A *et al.* Human recombinant soluble ACE2 in severe COVID-19. Lancet Respir Med. 8(11):1154-1158 (2020).

5. Khan A *et al.* A pilot clinical trial of recombinant human angiotensin-converting enzyme 2 in acute respiratory distress syndrome. *Crit Care.* 21(1):234 (2017).

6. Batlle D, Wysocki J, Soler MJ, Ranganath K, Angiotensin-converting enzyme 2: enhancing the degradation of angiotensin II as a potential therapy for diabetic nephropathy. *Kidney Int.* 81(6):520-8 (2012).

7. Evans CE, Miners JS, Piva G, Willis CL, Heard DM, Kidd EJ, Good MA, Kehoe PG. ACE2 activation protects against cognitive decline and reduces amyloid pathology in the Tg2576 mouse model of Alzheimer's disease. *Acta Neuropathol.* 2020 139(3):485-502.

8. Erster O *et al.* Site-specific targeting of antibody activity in vivo mediated by disease-associated proteases. *J Control Release.* 161(3):804-12 (2012).

9. Zhong JC *et al.* Targeting the apelin pathway as a novel therapeutic approach for cardiovascular diseases. *Biochim Biophys Acta Mol Basis Dis.* 1863(8):1942-1950 (2017).

10. Vickers C *et al.* Hydrolysis of biological peptides by human angiotensin-converting enzyme-related carboxypeptidase. *J Biol Chem.* 277(17):14838-43 (2002).

11. Wang W *et al.* Angiotensin-Converting Enzyme 2 Metabolizes and Partially Inactivates Pyr-Apelin-13 and Apelin-17: Physiological Effects in the Cardiovascular System. *Hypertension.* 68(2):365-77 (2016).

12. Yavuz YC *et al.* Role of Circulating Serum Apelin-13 Levels in Glomerulonephritis: A Pilot Study. *J Clin Exp Nephrol* 1:2. DOI: 10.21767/2472-5056.100002 (2015).

13. Chappell MC. Biochemical evaluation of the renin-angiotensin system: the good, bad, and absolute? *Am J Physiol Heart Circ Physiol.* 2016 310(2):H137-52.

14. Sullivan JC, Rodriguez-Miguelez P, Zimmerman MA, Harris RA. Differences in angiotensin (1-7) between men and women. *Am J Physiol Heart Circ Physiol.* 2015 308(9):H1171-6.

15. van Kats JP *et al.* Intrarenal angiotensin II: interstitial and cellular levels and site of production. *Kidney Int.* 60(6):2311-7 (2001).

16. Chao G *et al.* Isolating and Engineering Human Antibodies Using Yeast Surface Display. *Nat Protoc.* 1(2):755-68 (2006).

17. Cherf GM, Cochran JR, Applications of Yeast Surface Display for Protein Engineering. *Methods Mol Biol.* 1319:155-75 (2015).

18. Towler P *et al.* ACE2 X-ray structures reveal a large hinge-bending motion important for inhibitor binding and catalysis. *J Biol Chem.* 279(17):17996-8007 (2004).

19. Nov Y, When second best is good enough: another probabilistic look at saturation mutagenesis. *Appl Environ Microbiol.* 78(1):258-62 (2012).

20. Yan R, Zhang Y, Li Y, Xia L, Guo Y, Zhou Q, Structural basis for the recognition of SARS-CoV-2 by full-length human ACE2. *Science.* 367(6485):1444-1448 (2020).

21. Chan KK *et al.* Engineering human ACE2 to optimize binding to the spike protein of SARS coronavirus 2. *Science.* 69(6508):1261-1265 (2020).

22. van Kats JP, Schalekamp MA, Verdouw PD, Duncker DJ, Danser AH, Intrarenal angiotensin II: interstitial and cellular levels and site of production. *Kidney Int.* 60(6):2311-7 (2001).

23. Yavuz YC *et al.* Role of Circulating Serum Apelin-13 Levels in Glomerulonephritis: A Pilot Study. *J Clin Exp Nephrol* 1:2. DOI: 10.21767/2472-5056.100002 (2015).

24. Lubbe L, Cozier GE, Oosthuizen D, Acharya KR, Sturrock ED, ACE2 and ACE: structure-based insights into mechanism, regulation and receptor recognition by SARS-CoV. *Clin Sci (Lond).* 134(21):2851-2871 (2021).

25. Sodhi CP *et al.* Attenuation of pulmonary ACE2 activity impairs inactivation of des-Arg9 bradykinin/BKB1R axis and facilitates LPS-induced neutrophil infiltration. *Am J Physiol Lung Cell Mol Physiol.* 314(1):L17-L31 (2018).

26. Shusta EV, Kieke MC, Parke E, Kranz DM, Wittrup KD, Yeast polypeptide fusion surface display levels predict thermal stability and soluble secretion efficiency. *J Mol Biol.* 292(5):949–56 (1999).

27. Burns ML *et al.* Directed evolution of brain-derived neurotrophic factor for improved folding and expression in Saccharomyces cerevisiae. *Appl Environ Microbiol.* 80(18):5732–42 (2014).

28. Olsen MJ *et al.* Function-based isolation of novel enzymes from a large library. *Nat Biotechnol.* 18(10):1071-1074 (2000).

29. Yi L *et al.* Engineering of TEV protease variants by yeast ER sequestration screening (YESS) of combinatorial libraries. *Proc Natl Acad Sci U S A.* 110(18):7229-7234 (2013).

30. Holstein JM, Gylstorff C, Hollfelder F, Cell-free Directed Evolution of a Protease in Microdroplets at Ultrahigh Throughput. *ACS Synth Biol.* 10(2):252-257 (2021).